

DR ZANE B. ANDREWS (Orcid ID : 0000-0002-9097-7944)

PROFESSOR JEFFREY S DAVIES (Orcid ID : 0000-0002-4234-0033)

Article type : Original Article

Calorie restriction activates new adult born olfactory-bulb neurones in a ghrelin-dependent manner but acyl-ghrelin does not enhance sub-ventricular zone neurogenesis

Michael Ratcliff¹, Daniel Rees^{1*}, Scott McGrady¹, Luke Buntwal¹, Amanda K. E. Hornsby¹, Jaqueline Bayliss², Brianne A. Kent³, Timothy Bussey⁴, Lisa Saksida⁴, Amy L Beynon¹, Owain W Howell¹, Alwena H. Morgan¹, Y Sun⁵, Zane B. Andrews², Timothy Wells⁶, Jeffrey S. Davies^{1§}

¹Molecular Neurobiology, Institute of Life Sciences, School of Medicine, Swansea University, UK. SA28PP. ²Department of Physiology, Biomedical Discovery Unit, Monash University, Melbourne, Australia. ³Department of Medicine, Vancouver, University of British Columbia, Canada. ⁴Western University, London, Ontario, Canada. ⁵Department of Nutrition and Food Science, Texas A&M University, College Station, USA. ⁶School of Biosciences, Cardiff University, UK.

§Correspondence should be addressed to jeff.s.davies@swansea.ac.uk

*Current address: School of Management, Swansea University, Bay Campus, Swansea, SA1 8EN, UK

Keywords: Ghrelin, Neurogenesis, Olfactory bulb, Sub-ventricular zone, Calorie restriction

This is the author manuscript accepted for publication and has undergone full peer review but has not been through the copyediting, typesetting, pagination and proofreading process, which may lead to differences between this version and the [Version of Record](#). Please cite this article as [doi: 10.1111/JNE.12755](https://doi.org/10.1111/JNE.12755)

This article is protected by copyright. All rights reserved

Figures: 4

Supplementary figures: 5

Highlights

- Acyl-ghrelin receptor, GHSR, is not expressed in the SVZ
- Acyl-ghrelin does not modulate SVZ cell proliferation
- Acyl-ghrelin does not increase adult olfactory bulb neurogenesis
- Genetic ablation of ghrelin does not affect survival of new adult born neurones
- Acyl-ghrelin receptor, GHSR, is expressed in the olfactory bulb
- Calorie restriction activates new adult born neurones in a ghrelin-dependent manner

Dr Jeffrey S Davies,
Molecular Neurobiology,
Institute of Life Sciences,
School of Medicine,
Swansea University,
UK. SA2 8PP.
Tel: +44 (0)1792 602209
jeff.s.davies@swansea.ac.uk

Abstract

The ageing and degenerating brain show deficits in neural stem/progenitor cell (NSPC) plasticity that are accompanied by impairments in olfactory discrimination. Emerging evidence suggests that the gut-hormone ghrelin plays an important role in protecting neurones, promoting synaptic plasticity and increasing hippocampal neurogenesis in the adult brain. Here, we studied the role of ghrelin in modulating adult sub-ventricular zone (SVZ) NSPCs that give rise to new olfactory bulb (OB) neurones. We characterised the expression of the ghrelin receptor, growth hormone secretagogue receptor (GHSR), using an immuno-histochemical approach in GHSR-eGFP reporter mice to show that GHSR is expressed in several regions, including the OB, but not in the SVZ of the lateral ventricle. These data suggest that acyl-ghrelin does not mediate a direct effect on NSPC in the SVZ. Consistent with these findings, treatment with acyl-ghrelin or genetic silencing of GHSR did not alter NSPC proliferation within the SVZ. Similarly, using a BrdU pulse-chase approach we show that peripheral treatment of adult rats with acyl-ghrelin did not increase the number of new adult-born neurones in the granule cell

layer (GCL) of the OB. These data demonstrate that acyl-ghrelin does not increase adult OB neurogenesis. Finally, we studied whether elevating ghrelin indirectly, via calorie restriction (CR), regulated the activity of new adult-born cells in the OB. Overnight CR induced c-Fos expression in new adult-born OB cells, but not in developmentally born cells, whilst neuronal activity was lost following re-feeding. These effects were absent in ghrelin^{-/-} mice, suggesting that adult-born cells are uniquely sensitive to changes in ghrelin mediated by fasting and re-feeding. In summary, ghrelin does not promote neurogenesis in the SVZ and OB, however, new adult-born OB cells are activated by CR in a ghrelin-dependent manner.

Introduction

The generation of new adult-born neurones in the olfactory bulb (OB) continues throughout life and contributes to olfactory memory. The adult OB receives new neurones that originate from divided neural stem / progenitor cells (NSPCs) residing in the sub-ventricular zone (SVZ) adjacent to the lateral ventricles. Following NSPC division, the cells differentiate into immature neuroblasts and migrate along the rostral migratory stream (RMS) prior to integration with local OB circuitry¹. This process of adult OB neurogenesis (AORN) is regulated by several intrinsic and extrinsic factors including age, exercise, inflammation and glucocorticoids¹. However, the underlying mechanisms mediating this process are poorly understood.

Within the OB, new adult-born neurones promote olfactory memory and enhance the ability to discriminate distinct odours^{2,3}. AORN is also important for OB granule cell replacement and tissue maintenance⁴. Olfactory impairment has been reported as a prodromal indicator of several neurodegenerative diseases⁵. For example, deficits in olfactory discrimination (i.e the ability to distinguish odours) have been described in experimental neurodegenerative animal models and human Parkinson's disease⁶.

Ghrelin, an orexigenic gut hormone produced in response to calorie restriction, acts on the hypothalamus to stimulate the release of growth hormone (GH), and promote meal initiation and food intake. Emerging evidence suggests that acyl-ghrelin may also have important extra-

hypothalamic functions⁷, such as increasing olfactory sensitivity⁸ and regulating activity in brain regions involved in olfaction and appetitive behaviour⁹.

In the neurogenic niche of the hippocampus, acyl-ghrelin has been shown to increase cell proliferation¹⁰ and the number of new adult-born neurones in adult rodents¹¹. The ghrelin receptor, GHSR, which is expressed within the dentate gyrus of the hippocampus, mediates the pro-neurogenic effect of calorie restriction (CR)¹², as well as the increase in hippocampal neurogenesis and antidepressant-like effect following P7C3 treatment¹³. Moreover, ghrelin deficient mice are reported to have impaired cell proliferation in the SVZ that is normalised to wild-type levels with exogenous acyl-ghrelin treatment¹⁴. GHSR is the only molecularly identified receptor for ghrelin, mediating the central effects of this hormone on appetite, body weight and energy metabolism¹⁵. However, it is not known whether GHSR is expressed within the neurogenic niche of the SVZ or whether acyl-ghrelin modulates adult olfactory bulb neurogenesis (AOBN). Here, we aimed to determine the expression pattern of GHSR within the SVZ and whether ghrelin modulates AOBN.

In addition, as fasting and feeding increase¹⁶ and decrease olfactory sensitivity¹⁷, respectively, we sought to determine whether ghrelin modulates the fasting-induced activation of both new adult-born and developmentally-born OB neurones.

Materials and Methods

Animals and procedures

All experiments involving animals were performed with appropriate ethical approval. Mouse studies were performed at Cardiff University (GHSR-null, Ghrelin^{-/-}) and Monash University (GHSR-eGFP). Studies involving rats were performed at the University of Cambridge.

Mice

GHSR-eGFP mice. Adult male GHSR-eGFP reporter mice were housed at room temperature on a 12h light, 12h dark cycle (0700-1900h) with free access (*ad libitum*) to food and water. GHSR-eGFP reporter mice¹⁸ (n=6) were obtained from the Mouse Mutant Regional Resource Center at the University of California Davis, and the hemizygous mice back-crossed to C57BL/6J mice. GHSR-eGFP reporter mice were terminally anaesthetised and trans-cardially perfused with 4% paraformaldehyde (PFA) in 0.1M PBS. Whole brains were rapidly removed and post-fixed in ice cold 4% PFA for 24h at 4°C before being sunk in 30% sucrose. Finally, brains were transferred to PBS + 0.1% sodium azide (Sigma Aldrich, St Louis, USA) and stored at 4°C prior to analysis.

Brains were frozen using a fine powder of ground-up dry ice and mounted on a sliding sledge freezing microtome (Zeiss, Microm HM 450) using Jung's freezing medium. The thermostat was set to -30°C to ensure brains remained frozen. 30µm thick coronal sections cut along the entire rostral-caudal axis (bregma +5.345mm to -4.08) were collected in a 96-well plate (Nunc, nunclon surface) filled with PBS + 0.1% sodium azide and stored at 4°C until required. Ghser-eGFP mouse brains were also collected in a sagittal orientation (bregma +3.925 to -0.20).

Immunofluorescence for GHSR-GFP. All experiments were performed on free-floating tissue sections at room temperature, unless stated otherwise. A 1 in 6 series of coronal or sagittal brain sections were selected (minimum of 10 sections per mouse), transferred into a 24-well culture plate (Nunc, nunclon surface) and washed in PBS (Sigma Aldrich, St Louis, USA) three times for 5 minutes each. Tissue sections were then permeabilised in methanol (Fisher Scientific, Loughborough, UK) at -20°C for 2 minutes and washed (as before) in PBS. Non-specific binding sites were blocked with 5% normal goat serum (NGS) (Sigma Aldrich, St Louis, USA) in PBS + 0.1% triton x-100 (Sigma Aldrich, Gillingham, UK) (PBS-T) for 1h. Excess block was removed and tissue sections incubated with chicken anti-GFP (Chicken polyclonal, Abcam, Cambridge, UK, Ab13970), diluted 1:1000 in PBS-T, for 24h at 4°C. Primary antibody was omitted from the negative control. Sections were washed and incubated in goat anti-chicken Alexa-fluor 488 (Goat polyclonal, Life technologies, USA, A11039), diluted 1:500 in PBS-T, for 30 minutes in the dark. Finally, sections were washed, mounted onto Superfrost⁺ slides (Fisherbrand, Superfrost⁺ slides) and cover-slipped with vectashield (containing DAPI) (Vector Labs, Burlingame, USA) before being stored at 4°C. The slides were analysed by laser scanning confocal microscopy (Zeiss, LSM710) and Zen software (Zeiss, Zen 2010 edition) after 24h. Freely available GIMP v2.8 software was used to prepare tiled images of coronal and sagittal sections (www.gimp.org).

GHSR-null mice. For assessing exogenous acyl-ghrelin regulation of SVZ cell proliferation, homozygous male loxTB-GHSR mice (GHSR-null) (a gift from Prof Jeffrey Zigman, University of Texas Southwestern Medical Center, Dallas, TX) and W-T (C57BL/6J; W-T) controls (Harlan UK Ltd.) (14 weeks-old, n = 3 / group) were used¹⁹. The methodological and metabolic aspects of this study have previously been described²⁰. Briefly, mice were prepared with jugular vein cannulae attached to osmotic mini-pumps (Alzet model 2001) under isoflurane anesthesia. The mini-pumps delivered either vehicle or acyl-ghrelin (48µg/day; Phoenix Pharmaceuticals, USA) for 7 days. This treatment protocol was shown to increase abdominal adiposity via GHSR, but had no effect on body weight²⁰. Mice were euthanised by cervical dislocation and whole trunk

blood was collected into heparinized tubes for plasma separation by centrifugation at 4,000g for 10 minutes at 4°C. Whole brain was removed and immediately snap frozen on dry ice and stored at -80°C prior to analysis.

For analysis of Ki67, snap-frozen brains were sectioned at 10µm thickness using a cryostat (Leica) and mounted directly onto superfrost⁺ coated slides (VWR). A one-in-fifteen series of 10µm sections (150µm apart) from each animal, a minimum of 8 sections per mouse, was immunostained using rabbit anti-Ki67 (1:500, ab16667, Abcam) along with a biotinylated goat anti-rabbit for Ni-DAB based detection, as previously described¹¹. Cells were imaged by light microscopy (Nikon 50i) prior to quantification using Image J software.

A separate cohort of 19-week old male GHSR-null mice, derived from crosses between animals that were heterozygous for the GHSR-null allele and that had been backcrossed >10 generations onto a C57BL/6J genetic background, and WT littermate mice were housed under normal laboratory conditions (12 h light: 12 h dark, lights on at 06.00 h) (n=3/genotype). Mice were killed by cervical dislocation under terminal anaesthesia, whole brain was removed, immersed in 4% PFA for 24h at 4°C and cryoprotected in 30% sucrose prior to preparation of coronal sections (30µm) cut into a 1:12 series along the entire rostro-caudal extent of the brain using a freezing-stage microtome (MicroM, ThermoScientific) and collected for IHC. For DAB-immunohistochemical analysis of GHSR labelling, a minimum of 6 sections per mouse were washed in 0.1M PBS (2 × 10min) and 0.1M PBS-T (1 × 10min). Subsequently, endogenous peroxidases were quenched by washing in a PBS plus 1.5% H₂O₂ solution for 20min. Sections were washed again (as above) and incubated in 5% NDS in PBS-T for 1h. Sections were incubated overnight at 4°C with rabbit anti-GHSR1a (Phoenix Pharmaceuticals, H-001-62), diluted 1:2000 in PBS-T and 2% NGS solution. Another wash step followed prior to incubation with biotinylated goat anti-rabbit (1:400; Vectorlabs, USA) in PBS-T for 70min. The sections were washed and incubated in ABC (Vector- labs, USA) solution for 90min in the dark prior to another two washes in PBS, and incubation with 0.1 M sodium acetate pH6 for 10min. Immunoreactivity was developed in Nickel enhanced DAB solution followed by two washes in PBS. Sections were mounted onto superfrost⁺ slides (VWR, France) and allowed to dry overnight before being de-hydrated and de-lipified in increasing concentrations of ethanol. Finally, sections were incubated in histoclear (2 × 3min; National Diagnostics, USA) and coverslipped using entellan mounting medium (Merck, USA). Slides were allowed to dry overnight prior to imaging.

Calorie restriction in Ghrelin^{-/-} mice. Adult female homozygous ghrelin knockout (ghrelin^{-/-}) mice²¹ and their wild type (WT) littermates were derived from crosses between animals that were heterozygous for the ghrelin-null allele. These mice were backcrossed >10 generations on a C57BL/6J genetic background and acclimatized to being individually housed for 7 days under normal laboratory conditions (12h light, 12h dark cycle; 0700-1900h) prior to the onset of the study. Mice were divided into six groups (n=5-8/group) that included *ad-libitum* fed WT, calorie restricted (CR) WT, calorie restricted/re-fed (CR/RF) WT, *ad-libitum* fed ghrelin^{-/-}, CR ghrelin^{-/-} and CR/RF ghrelin^{-/-}. For the first 28 days of the study, mice were fed on an *ad-libitum* diet with daily injections (from days 1-4) of the thymidine analogue, BrdU (50mg/kg; i.p), to label actively dividing cells. On day 28, food was withdrawn at 17.30h from the CR and CR/RF mice. On the subsequent day, CR/RF mice were allowed to feed *ad-libitum* for 1h prior to all animals undergoing cervical dislocation whilst under terminal anaesthesia (~18h CR). Ghrelin^{-/-} mice have growth rates and appetite similar to WT littermates, with no impairment in hyperphagia after fasting^{21,22}. Similarly, adult ablation of ghrelin in mice does not impair growth nor appetite²³. Whole brains were removed, immersed in ice cold 4% PFA for 24h and cryoprotected in 30% sucrose. Coronal sections (30µm) were cut in a 1:12 series along the entire rostral-caudal axis of the olfactory bulb (bregma +5.345mm to +2.445mm) using a freezing stage microtome (MicroM, Thermo Scientific) and collected for IHC.

Quantification of BrdU⁺/c-Fos⁺: All IHC was performed on free-floating sections at room temperature, unless otherwise stated. A 1:6 series of 30µm sections (180µm apart) were washed three times in PBS for 5 min, permeabilised in methanol at -20°C for 2 min, and washed as before. DNA was denatured with 2M HCL for 30 min at 37°C prior to washing sections in 0.1M borate buffer (pH 8.5) for 10 minutes. Sections were washed, blocked with 5% normal goat serum (NGS) plus 5% bovine serum albumin (BSA) in PBS plus 0.1% Triton (PBS-T) for 60 min and incubated in a cocktail of primary antibodies that included rat anti-BrdU (1:400; MCA2060, ABD Serotec) and rabbit anti-c-Fos (1:1000; SC-52, Santa Cruz) in PBS-T overnight at 4°C. The primary antibody was omitted from the negative control.

Following primary antibody treatment, sections were washed, incubated with biotinylated goat anti-rat (1:400; BA-9400, Vector Labs) in PBS-T for 60 min in the dark and then washed as before. Similarly, secondary antibodies were also applied as a cocktail that included goat anti-rabbit (1:400; BA-1000, Vector Labs) and streptavidin AF-594 (1:500; S11227, Life Technologies) in PBS-T for 30 min. Following another wash, including one containing Hoechst nuclear stain, sections were mounted onto superfrost⁺ slides (VWR, France) and cover-slipped with prolong gold anti-fade solution (Life Technologies, USA).

Quantification of immunolabelled cells: A 1:6 series of 30µm sections (180µm apart) from each animal was analysed for immunoreactivity using an epi-fluorescent microscope system (Zeiss, Imager M1 with Axiocam MRm). Immunolabelled cells were manually counted bilaterally using a ×40 objective through the z-axis of the entire rostral-caudal extent of the dorsal granule cell layer (GCL), glomerular layer (GL), subependymal zone (SEZ) and the lateral olfactory tract body (LOT). Resulting numbers were divided by the total area measurement to give a count per pixel, which was converted into mm² and averaged for each brain. All analyses were performed blind to both genotype and treatment.

Rats

Adult male lister hooded rats (n=10/11 per group, weighing 250-300g; Harlan, Bicester, UK) were housed in groups of four and maintained at room temperature on a 12h light, 12h dark cycle (0700-1900h). These experimental procedures have previously been described¹¹. Briefly, from days 0-14, rats received daily intra-peritoneal injections of acyl-ghrelin (Phoenix Pharmaceuticals, 031-31) or saline (10µg/kg body weight) with BrdU injections (50mg/kg) on days 5-8. On day 29, rats were terminally anaesthetised, trans-cardially perfused with 4% PFA and brains were removed for immersion fixation and cryoprotection (as before). Analysis of adult hippocampal neurogenesis (AHN) in these rats demonstrated that acyl-ghrelin significantly increased the number of new adult born neurones¹¹.

Double immunofluorescence for BrdU/NeuN: A 1 in 6 series of coronal OB brain sections (bregma +5.345mm to +2.445) were transferred into a 24-well culture plate and washed in PBS, permeabilised in methanol at -20°C for 2 minutes and washed in PBS as before. DNA was denatured using 2M hydrochloric acid (HCL) (Fisher Scientific, Loughborough, UK) and incubated at 37°C for 30 minutes. Excess HCL was removed and the sections washed in 0.1M borate buffer, pH 8.5, for 10 minutes to neutralise the remaining HCL. Tissue sections were then washed, blocked with 5% NGS diluted in PBS-T for 1h and incubated with rat anti-BrdU (Rat monoclonal, ABD Serotec, Oxfordshire, UK, MCA2060), diluted 1:3000 in PBS-T for 24h at 4°C. The primary antibody was omitted from the negative control. Sections were washed and incubated with biotinylated goat anti-rat (Goat polyclonal, Vector labs, Burlingham, USA, BA-9400), diluted 1:400 in PBS-T for 1h in the dark. Tissue sections were subsequently washed, incubated in streptavidin AF594 (Life technologies, Eugene, USA, S11227), diluted 1:500 in PBS-T for 30 minutes and washed as before. Sections were then incubated in mouse anti-NeuN (Mouse monoclonal, EMD Millipore, Massachusetts, USA, MAB377), diluted 1:1000 in PBS-T for 1h. The negative control contained PBS-T. Tissue sections were then washed and incubated in goat anti-mouse AF 488 diluted 1:500 in PBS-T for 30 minutes, prior to being washed with

Hoescht, diluted 1:10000 in PBS, for 5 minutes. Finally, sections were washed, mounted onto Superfrost⁺ slides and cover-slipped with prolong gold anti-fade reagent, prior to storage at 4°C.

Quantification of BrdU⁺: Image J software (version 1.47) was used to quantify the number of new adult-born cells in the dorsal and ventral granular cell layer (GCL) of the OB. Images taken by the fluorescent microscope were inverted and unsharp-masked, using a radius of 10.0 pixels and a mask weight of 0.60. The polygon tool was then used to draw around the granular cell layer and the total area measured. Each image's threshold was individually optimised, typically ranging from 0.100 – 0.180. The particle size was set to 20-300 pixel² and circularity at 0.0-1.0. Resulting numbers were divided by the total area measurement to give a count per pixel, which was then averaged for each brain.

Quantification of BrdU⁺/NeuN⁺: To quantify the number of new adult-born neurons in the dorsal and ventral granular cell layer of the OB, BrdU⁺/NeuN⁺ immunoreactive cells were manually counted through the z-axis of the entire rostral-caudal extent of the OB. Resulting numbers were divided by the area of the z-stack to give a count per pixel, which was then averaged for each brain.

Microscopy

Tissue sections were analysed using a fluorescent microscope (Zeiss, Imager M1 with Axioacam MRm) with Axiovision software (version 4.6) and a laser scanning confocal microscope (Zeiss, LSM 710) with Zen software (Zen 2010 edition). Images were collected using ×4, ×10 and ×40 objectives. BrdU⁺/NeuN⁺ immunoreactive newborn adult neurones, in the dorsal and ventral GCL, were imaged using a ×40 oil immersion objective. A z-stack consisting of 21-25 tissue slices at 0.7µm intervals (14.0-16.8µm range) were taken throughout the rostral-caudal extent of the OB.

All experiments and analyses were performed blind to genotype and treatment.

Statistical Analysis

Statistical analyses were performed using GraphPad Prism 6.0 for Mac (GraphPad Software, San Diego, CA). Statistical significance was assessed by an unpaired two-tailed Student's *t*-test or one-way ANOVA with Bonferroni's *post-hoc* test. Where there was more than one variable a two-way ANOVA with Tukey's multiple comparisons test was used or by a Kruskal-Wallis test followed by a Dunn's multiple comparisons test when a normal distribution of data could not be

assumed. Data are presented as a mean \pm SEM. *, $P < 0.05$; **, $P < 0.01$; ***, $P < 0.001$ and ****, $P < 0.0001$ were considered statistically significant.

Results

GHSR is expressed in the adult OB but not in the SVZ

The expression of GHSR was assessed to determine whether ghrelin could directly influence the proliferation of NSPCs in the SVZ. To achieve this aim we used GHSR-eGFP reporter mice to show that eGFP immunoreactivity was present within the anterior olfactory nucleus (AON) and orbital and motor orbital cortex in the caudal OB (figure 1i). Immunoreactivity was observed within the anterior cingulate cortex, motor cortex and lateral septal nucleus (figure 1ii). Sagittal sections revealed strong immunoreactivity in the anterior amygdala area, granule cell layer of the hippocampal dentate gyrus (DG) and the medial amygdala nucleus (figure 1iii). Notably, staining was absent within the lateral lining of the SVZ in tissue sectioned in both a coronal and sagittal orientation (figure 1iiD and iiiC). To determine whether the GHSR-eGFP immunoreactivity was similar to that observed with GHSR1a antisera, we performed IHC using a rabbit anti-GHSR1a antibody on adult WT and GHSR-null mouse brain tissue. These analyses revealed a similar pattern of immunoreactivity on both WT and GHSR-null tissues, including the SVZ (figure S1), suggesting a lack of binding specificity for the GHSR1a antigen. These data suggest that ghrelin may be involved in olfactory function but not through direct modulation of NSC's lining the lateral wall of the SVZ.

Acyl-ghrelin does not increase cell proliferation in the adult SVZ

The proliferative effect of ghrelin and GHSR-agonists have been widely reported within CNS and peripheral tissues²⁴⁻²⁶. A recent study reported that ghrelin promoted proliferation of cells within the SVZ¹⁴. Here, we took advantage of genetically modified mice to analyse the effect of acyl-ghrelin treatment on SVZ cell proliferation in adult WT and GHSR-null mice, where GHSR is transcriptionally silenced. Using the mitotic marker, Ki67, we report that acyl-ghrelin treatment had no effect on the number of proliferating cells within the SVZ niche in WT mice (figure 2, $P = > 0.99$). Similarly, transcriptional silencing of GHSR did not affect the rate of SVZ cell division in vehicle (WT veh vs GHSR-null veh, $P = 0.6388$) or acyl-ghrelin treated mice (GHSR-null veh vs GHSR-null acyl-ghrelin, $P = 0.0944$). The low number of replicates means that the statistical analysis is of low power, however, the data suggest that acyl-ghrelin does not regulate cell proliferation in the adult mouse SVZ and that genetic silencing of GHSR does not decrease cell division in this niche.

Acyl-ghrelin does not increase the number of new adult-born olfactory bulb neurones

We recently showed that treatment with acyl-ghrelin increased adult hippocampal neurogenesis (AHN) in adult rats¹¹. To determine whether acyl-ghrelin treatment modulates AOBN in a similar way to AHN, we quantified the number of new adult-born neurones in the OB of adult rats from the same study. Using OB tissue from the same rats whereby acyl-ghrelin increased AHN provides us with valuable experimental controls. We show there was no significant difference in the number of new adult-born cells (BrdU⁺/NeuN⁺) in the GCL of the OB following acyl-ghrelin treatment compared to saline treatment (figure 3G, $P = 0.8482$). Similarly, no differences were observed in the number of new adult-born neurones (BrdU⁺/NeuN⁺) (figure 3H, $P = 0.7388$) or in the rate of neurone differentiation (figure 3I, $P = 0.6870$).

Calorie restriction induces activation of new adult-born OB cells in a ghrelin-dependent manner

To determine whether a CR-mediated increase in endogenous acyl-ghrelin was able to increase the expression of the proto-oncogene, c-Fos, in new adult-born OB cells, we analysed the number of active c-Fos⁺ cells within the GCL, GL, SEZ and LOT in WT and ghrelin^{-/-} mice. A two-way ANOVA revealed a statistically significant main effect of treatment on BrdU⁺ ($p = 0.0031$) and BrdU⁺/c-Fos⁺ ($p = 0.0487$) cells within the GCL. Comparatively, genotype and the interaction (treatment and genotype) showed a significant effect on c-Fos⁺ ($p = 0.0001$ and 0.017 , respectively) and BrdU⁺/c-Fos⁺ ($p = 0.0002$ and 0.00021 , respectively) cells within the GCL. Outside of the GCL, a significant main effect of treatment was reported in BrdU⁺/c-Fos⁺ cells of the SEZ ($p = 0.0118$) and BrdU⁺ cells of the LOT ($p = 0.0075$). No increase was observed within the GL (Table S1).

A Tukey post hoc test revealed a reduction in the number of new adult-born cells (BrdU⁺) in CR/re-fed (CR/RF) ghrelin^{-/-} mice, compared with CR ghrelin^{-/-} mice (figure 4C, $P = 0.0086$) within the GCL. Furthermore, there was an increased number of activated cells (c-Fos⁺) in CR WT mice, compared with *ad libitum* WT ($P = 0.0258$) and CR/RF WT ($P = 0.0043$) mice. Notably, CR also increased activated cells in WT relative to CR ghrelin^{-/-} mice ($P < 0.0001$) within the GCL (figure 4D). Further analysis revealed that the number of active new adult-born cells (BrdU⁺/c-Fos⁺) was increased in CR WT mice compared with CR/RF WT ($P = 0.0169$) and CR ghrelin^{-/-} mice ($p < 0.0001$) within the GCL (figure 4E). Whereas, there were very few active developmentally born cells (BrdU⁺/c-Fos⁺) and these cells were not significantly affected by treatment or genotype (figure 4F). Outside of the GCL, the number of active new adult-born cells (BrdU⁺/c-Fos⁺) was reduced in CR ghrelin^{-/-} mice, compared with *ad-libitum* fed ghrelin^{-/-} mice ($P = 0.0169$) within the SEZ. No significant differences were reported in the other regions tested (Table S1). There was no significant difference in body weight change in ghrelin^{-/-} mice relative to WT mice in either of the groups (Two-way ANOVA; main effect of genotype, $P = 0.9335$; main

effect of feeding pattern, $P = 0.0049$; main effect of interaction (feeding pattern vs genotype), $P = 0.3469$). Collectively, these data suggest that CR increases the activation of new adult-born cells in a ghrelin-dependent manner.

Discussion

The generation of new OB neurones in the adult brain is important for olfactory discrimination, a process that is impaired in ageing and several neurodegenerative disorders. Here, we tested the hypothesis that ghrelin is an important regulator of AOBN. First, we characterised expression of GHSR in the adult mouse brain. Numerous studies have attempted to characterise the expression pattern of GHSR in several species, including mouse, rat and lemur^{27–30}, though the lack of reliable anti-GHSR antibodies have limited progress. More recently, a report using the GHSR-eGFP mouse and in situ hybridisation histochemistry demonstrated GHSR expression within the OB, hippocampus and hypothalamic nuclei¹⁵. Furthermore, Cre-activity in *Ghsr*-IRES-Cre/ROSA26-ZsGreen reporter mice was also reported in the main and accessory OB³¹.

Here, using adult GHSR-eGFP mice, we report GHSR immunoreactivity in the MCL, AON and orbital and motor orbital cortices of the OB, as well as within the anterior cingulate cortex, motor cortex, lateral septal nucleus, entopeduncular nucleus, hippocampus and the medial amygdaloid nucleus. However, GHSR was not expressed within the neurogenic niche of the SVZ in GHSR-eGFP reporter mice. Indeed, this finding is consistent with previous studies that do not report GHSR immunoreactivity within the SVZ niche. Together, these findings suggest that ghrelin does not mediate direct effects on NSPC proliferation.

As eGFP immunoreactivity in this transgenic model may correspond to two structurally different receptors, GHSR1a, which encodes the functional receptor, and the truncated GHSR1b, generated from alternative splicing of GHSR, we sought to identify GHSR1a expressing cells using antisera raised against GHSR1a. The specificity of polyclonal antibodies used to characterise GHSR within the adult brain remains unclear. Li *et al.*¹⁴ reported GHSR expression within the adult mouse neurogenic niche of the SVZ using immuno-fluorescence with the rabbit anti-GHSR1a antibody (Phoenix Pharmaceuticals, H-001-62), diluted 1:500. In our study, using the same antibody, IHC in brain tissue from adult GHSR-null and WT mice revealed detectable immunoreactivity in tissue from both genotypes. Our data suggest that the rabbit anti-GHSR antibody resulted in non-specific staining within the SVZ and cingulate cortex (figure S1), preventing its use to determine GHSR1a expression in this context. Combined, these studies suggest that the ghrelin receptor is not expressed in the SVZ, and thus does not directly modulate NSPC proliferation.

To determine whether ghrelin induces cell proliferation within the SVZ we treated GHSR-null and wild-type mice for 7-days with acyl-ghrelin. Subsequent analysis revealed no effect of genotype or treatment on the number of dividing Ki67⁺ cells in the SVZ. In contrast, a previous study reported that ghrelin^{-/-} mice had a reduced number of proliferating NSPCs, migrating neuroblasts and OB interneurons, that could be restored to WT levels by intraperitoneal administration of acyl-ghrelin¹⁴. Several differences between the two experimental procedures might account for the contrasting results. For example, Li et al. used 8-9 week old WT and ghrelin^{-/-} mice that received acyl-ghrelin (80 µg/kg) via intraperitoneal injection, once daily for 8 consecutive days. Whereas, in our study 14-week old WT and GHSR-null mice were given acyl-ghrelin (48 µg/day) via intravenous mini-pump. Therefore, inconsistencies between studies may be attributable to genetic background, the physiological dose or the route of administration of acyl-ghrelin.

Next, using a BrdU pulse-chase approach we determined the effect of exogenous acyl-ghrelin treatment on the maturation and survival of new adult-born neurones in the rat OB. Consistent with our previous cell proliferation analysis in mice, acyl-ghrelin did not increase in the number of new adult-born BrdU⁺ cells or BrdU⁺/NeuN⁺ neurones in the GCL of the OB. Furthermore, no differences were observed in the rate of neuronal differentiation. Notably, we have previously reported that adult hippocampal neurogenesis was significantly increased by acyl-ghrelin in these rats¹¹. The high level of GHSR expression within hippocampal neurogenic niche¹² and its absence in the SVZ niche is likely responsible for this effect. These data provide compelling evidence that acyl-ghrelin does not promote AOBN.

Numerous studies have suggested that ghrelin plays an important role in olfactory-related behaviours including odour discrimination and sensitivity^{8,32,33}. Loch *et al.* reported an increased responsiveness of the mouse olfactory epithelium following nasal application of ghrelin. This resulted in a higher reactivity of olfactory sensory neurones within the olfactory epithelium, which in turn, increased the activity of receptor-specific glomeruli. GHSR expression on the surface of olfactory sensory neurones suggest that ghrelin and GHSR may play an important role in enhancing neuronal responsiveness and olfaction. However, the underlying mechanism by which acyl-ghrelin enhances olfaction remains elusive and it is unclear if new adult-born OB neurones are involved in this physiology.

As acyl-ghrelin is known to regulate both olfaction and appetite we sought to determine whether new adult-born OB neurones are activated by CR in a ghrelin-dependent manner. Our data demonstrate that overnight CR activated new adult-born cells in the OB. Re-feeding for one hour returned the number of c-Fos positive cells to baseline, suggesting that the new adult-born

cells are sensitive to feeding status. Notably, this CR effect was absent in ghrelin^{-/-} mice demonstrating that the activation of new adult-born cells was dependent upon intact ghrelin signalling. Furthermore, there was no CR-mediated activation of developmentally-born cells (BrdU⁺/c-Fos⁺) in the GCL of the OB indicating that adult-born neurones are uniquely responsive to acute changes in food intake. Therefore, we confirm that CR activates new adult-born OB cells in a ghrelin-dependent manner. This finding provides further support for ghrelin acting as a mediator of CR-associated physiology, including, neuroprotection³⁴, anti-anxiety³⁵, hippocampal neurogenesis and cognitive enhancement¹², and glycemic regulation³⁶.

Although the relationship between hunger stimulation and olfaction has been long recognised, a molecular mechanism relating the two processes has not been determined³⁷. Soria-Gomez *et al.* observed that cortical feedback projections to the OB crucially regulate food intake, possibly through cannabinoid type-1 receptor (CB1R) signalling. The endocannabinoid system, in particular CB-1Rs, promoted food intake in fasted mice by increasing odour detection. Notably, ghrelin's orexigenic effect is lost in CB-1R knock-out mice³⁸. Although the relationship between ghrelin and the endocannabinoid system in the OB is unknown, both GHSR and CB-1R are GPCRs known to form homo- and heterodimers (or higher-order oligomers) as part of their normal trafficking and function^{39,40}. Therefore, heterodimerisation of CB-1R and GHSR may be important in linking ghrelin to adult-born OB neurones and olfaction.

Several questions remain unanswered, including whether ghrelin alters the electrophysiological properties and/or directly activates GCs in the OB to enhance odour discrimination. As new adult-born OB cells enhance the odour-reward association³, further work is needed to determine whether the ghrelin-induced intake of rewarding foods⁴¹ requires signalling via new neurones in the OB. Similarly, it is not known whether ghrelin can increase appetite and improve olfaction in the absence of new adult-born OB cells.

In summary, these data demonstrate that while ghrelin does not increase SVZ-OB neurogenesis, it does mediate the CR-induced activation of new adult-born OB cells. We speculate that ghrelin modulates new OB neurone activity to integrate olfactory responses with nutritional status.

Figure legends

Figure 1. Characterisation of GHSR1a in the adult GHSR1a-eGFP mouse brain.

(i). GHSR1a-eGFP immunoreactivity is present within the orbital and motor orbital cortex and the anterior olfactory nucleus. CTX, cortex; AON, anterior olfactory nucleus.

(ii). Collage of coronal mouse sections (A). Inset images of GHSR1a-eGFP immunoreactivity in anterior cingulate cortex dorsal (B), anterior cingulate cortex (C) and lateral septal nucleus (E). GHSR1a-eGFP immunoreactivity is absent in the lateral lining of the SVZ (D).

(iii). Collage of sagittal mouse sections (A). Inset images of GHSR1a-eGFP immunoreactivity in primary motor cortex (B), anterior amygdala area (D), dorsal granule cell layer of the dentate gyrus (E), ventral dentate gyrus (F) and medial amygdalar nucleus (posterodorsal)(G). GHSR1a-eGFP immunoreactivity is absent within the lateral lining of the SVZ (C).

Montage image scale bar = 200µm. Inset image scale bar = 50µm.

Figure 2. Acyl-ghrelin treatment does not increase cell proliferation in the SVZ of adult wild-type or GHSR-null mice. (A) GHSR-null and WT littermate mice were treated for 7-days with either saline or acyl-ghrelin (48ug/day i.v) via osmotic mini-pump before brains were collected and Ki67 immunoreactivity quantified throughout the rostro-caudal extent of the SVZ. (B) Total number of Ki67⁺ cells did not change following acyl-ghrelin treatment in either WT or GHSR-null mice. Data are mean +/- SEM, n=3 mice per group. Statistical analysis performed by Kruskal-Wallis test ($P = 0.2087$) followed by a post-hoc Dunn's multiple comparison test.

Figure 3. Exogenous acyl-ghrelin does not increase the number of new adult born neurones in the granule cell layer of the rat olfactory bulb. (A) Experimental paradigm. (B) Collage image of the rat olfactory bulb. Representative images of BrdU (red) and NeuN (green) in (C) dorsal granule cell layer (GCL) and (D) ventral GCL of the OB. Scale bar = 200µm. Representative images of new adult-born neurones co-expressing NeuN⁺ and BrdU⁺ (yellow) in (E) dorsal GCL and (F) ventral GCL. Scale bar = 50µm. Quantification of new adult-born OB cells (G) ($P = 0.8482$), new adult-born neurones (H) ($P = 0.7388$) and % neuronal differentiation (I) ($P = 0.6870$) after acyl-ghrelin or saline treatment. Data are mean +/- SEM. Statistical analysis was performed by two-tailed unpaired Student's *t*-test. $P < 0.05$ considered significant, ns = not significant. n = 11 rats per group.

Figure 4. New adult-born OB cells are activated by calorie restriction in a ghrelin-dependent manner. (A) Schematic of experimental paradigm. (B) New adult-born active neurone (yellow; scale bar = 25µm) co expressing BrdU (green) and c-Fos (red) in the GCL of the OB. Scale bar = 50µm. Quantification of (C) new adult-born cells (BrdU⁺), (D) active cells (c-Fos⁺), (E) active new adult-born cells (BrdU⁺/c-Fos⁺) and (F) active developmentally born cells (BrdU/c-Fos⁺) in the GCL of the OB. (G) Representative images of new adult-born cells (BrdU⁺; green), active cells (c-Fos⁺; red) and active new adult-born cells (BrdU⁺/CFos⁺; yellow in merged image). Arrows

correspond to new BrdU⁺/c-Fos⁺ cells, whilst arrowheads represent active new adult-born BrdU⁺/c-Fos⁺ cells. Scale bar = 50µm. Statistical analysis was performed by two-way ANOVA with Tukey post hoc test. * P ≤ 0.05, ** P ≤ 0.01, **** P ≤ 0.0001. All data shown are mean +/- SEM; n = 5-8 rats per group. AL (ad-libitum), CR (calorie restriction), CR/RF (calorie restriction / re-fed), WT (wild-type), GKO (ghrelin^{-/-}).

References

1. Lledo, P.-M., Alonso, M. & Grubb, M. S. Adult neurogenesis and functional plasticity in neuronal circuits. *Nat. Rev. Neurosci.* **7**, 179–93 (2006).
2. Alonso, M. *et al.* Activation of adult-born neurons facilitates learning and memory. *Nat. Neurosci.* (2012). doi:10.1038/nn.3108
3. Grelat, A. *et al.* Adult-born neurons boost odor–reward association. *Proc. Natl. Acad. Sci.* **201716400** (2018). doi:10.1073/pnas.1716400115
4. Imayoshi, I. *et al.* Roles of continuous neurogenesis in the structural and functional integrity of the adult forebrain. **11**, 1153–1161 (2008).
5. Meshulam, R. I., Moberg, P. J., Mahr, R. N. & Doty, R. L. Olfaction in Neurodegenerative Disease. *Arch. Neurol.* **55**, 84 (1998).
6. Boesveldt, S. *et al.* A comparative study of odor identification and odor discrimination deficits in Parkinson's disease. *Mov. Disord.* **23**, 1984–1990 (2008).
7. Andrews, Z. B. The extra-hypothalamic actions of ghrelin on neuronal function. *Trends Neurosci.* **34**, 31–40 (2011).
8. Tong, J. *et al.* Ghrelin Enhances Olfactory Sensitivity and Exploratory Sniffing in Rodents and Humans. *J. Neurosci.* **31**, 5841 LP-5846 (2011).
9. Malik, S., McGlone, F., Bedrossian, D. & Dagher, A. Ghrelin Modulates Brain Activity in Areas that Control Appetitive Behavior. *Cell Metab.* **7**, 400–409 (2008).
10. Zhao, Z. *et al.* Ghrelin administration enhances neurogenesis but impairs spatial learning and memory in adult mice. *Neuroscience* **257**, 175–85 (2014).
11. Kent, B. A. *et al.* The orexigenic hormone acyl-ghrelin increases adult hippocampal neurogenesis and enhances pattern separation. *Psychoneuroendocrinology* **51**, 431–439 (2015).
12. Hornsby, A. K. E. *et al.* Short-term calorie restriction enhances adult hippocampal neurogenesis and remote fear memory in a Ghrelin-dependent manner. *Psychoneuroendocrinology* **63**, 198–207 (2016).
13. Walker, a K. *et al.* The P7C3 class of neuroprotective compounds exerts antidepressant efficacy in mice by increasing hippocampal neurogenesis. *Mol. Psychiatry* **1–9** (2014).

doi:10.1038/mp.2014.34

14. Li, E. *et al.* Ghrelin stimulates proliferation, migration and differentiation of neural progenitors from the subventricular zone in the adult mice. *Exp. Neurol.* **252**, 75–84 (2014).
15. Mani, B. K. *et al.* Neuroanatomical characterization of a growth hormone secretagogue receptor-green fluorescent protein reporter mouse. *J. Comp. Neurol.* **3666**, 3644–3666 (2014).
16. Goetzl, F. & Stone, F. Diurnal variations in acuity of olfaction and food intake. *Gastroenterology* **9**, 444–453 (1947).
17. Aimé, P. *et al.* Fasting increases and satiation decreases olfactory detection for a neutral odor in rats. *Behav. Brain Res.* **179**, 258–264 (2007).
18. Reichenbach, A., Steyn, F. J., Sleeman, M. W. & Andrews, Z. B. Ghrelin receptor expression and colocalization with anterior pituitary hormones using a GHSR-GFP mouse line. *Endocrinology* **153**, 5452–5466 (2012).
19. Zigman, J. M. *et al.* Mice lacking ghrelin receptors resist the development of diet-induced obesity. *J. Clin. Invest.* **115**, 3564–3572 (2005).
20. Davies, J. S. *et al.* Ghrelin induces abdominal obesity via GHS-R-dependent lipid retention. *Mol. Endocrinol.* **23**, 914–24 (2009).
21. Sun, Y., Ahmed, S. & Smith, R. G. Deletion of ghrelin impairs neither growth nor appetite. *Mol. Cell. Biol.* **23**, 7973–7981 (2003).
22. Wortley, K. E. *et al.* Genetic deletion of ghrelin does not decrease food intake but influences metabolic fuel preference. *Proc. Natl. Acad. Sci.* **101**, 8227–8232 (2004).
23. McFarlane, M. R., Brown, M. S., Goldstein, J. L. & Zhao, T. J. Induced ablation of ghrelin cells in adult mice does not decrease food intake, body weight, or response to high-fat diet. *Cell Metab.* **20**, 54–60 (2014).
24. Zhang, W., Hu, Y., Lin, T. R., Fan, Y. & Mulholland, M. W. Stimulation of neurogenesis in rat nucleus of the solitary tract by ghrelin. **26**, 2280–2288 (2005).
25. Zhang, W. *et al.* Ghrelin stimulates neurogenesis in the dorsal motor nucleus of the vagus. **3**, 729–737 (2004).
26. Moon, M., Hwang, L. & Park, S. Ghrelin Regulates Hippocampal Neurogenesis in Adult Mice. *Endocr. J.* **56**, 525–531 (2009).
27. Guan, X. *et al.* Distribution of mRNA encoding the growth hormone secretagogue receptor in brain and peripheral tissues. *Mol. Brain Res.* **48**, 23–29 (1997).
28. Mitchell, V. *et al.* Comparative distribution of mRNA encoding the growth hormone secretagogue-receptor (GHS-R) in *Microcebus murinus* (Primate, Lemurian) and rat forebrain and pituitary. *J. Comp. Neurol.* **429**, 469–489 (2000).

- 578 29. Sun, Y., Garcia, J. M. & Smith, R. G. Ghrelin and Growth Hormone Secretagogue Receptor
579 Expression in Mice during Aging. *Endocrinology* **148**, 1323–1329 (2007).
- 580 30. Zigman, J. M., Jones, J. E., Lee, C. E., Saper, C. B. & Elmquist, J. K. Expression of ghrelin
581 receptor mRNA in the rat and the mouse brain. *J. Comp. Neurol.* **494**, 528–548 (2006).
- 582 31. Mani, B. K. *et al.* The role of ghrelin-responsive mediobasal hypothalamic neurons in
583 mediating feeding responses to fasting. *Mol. Metab.* **6**, 882–896 (2017).
- 584 32. Loch, D., Breer, H. & Strotmann, J. Endocrine Modulation of Olfactory Responsiveness:
585 Effects of the Orexigenic Hormone Ghrelin. *Chem. Senses* **40**, 469–479 (2015).
- 586 33. Prud'homme, M. J. *et al.* Nutritional status modulates behavioural and olfactory bulb Fos
587 responses to isoamyl acetate or food odour in rats: roles of orexins and leptin.
588 *Neuroscience* **162**, 1287–1298 (2009).
- 589 34. Bayliss, J. *et al.* Ghrelin-AMPK signalling mediates the neuroprotective effects of Calorie
590 Restriction in Parkinson's Disease. *J. Neurosci.* **36**, 3049–3063 (2016).
- 591 35. Lutter, M. *et al.* The orexigenic hormone ghrelin defends against depressive symptoms of
592 chronic stress. *Nat. Neurosci.* **11**, 10–11 (2008).
- 593 36. Zhao, T.-J. *et al.* Ghrelin O-acyltransferase (GOAT) is essential for growth hormone-
594 mediated survival of calorie-restricted mice. *Proc. Natl. Acad. Sci. U. S. A.* **107**, 7467–72
595 (2010).
- 596 37. Soria-Gómez, E. *et al.* The endocannabinoid system controls food intake via olfactory
597 processes. *Nat. Neurosci.* (2014). doi:10.1038/nn.3647
- 598 38. Kola, B. *et al.* The orexigenic effect of ghrelin is mediated through central activation of the
599 endogenous cannabinoid system. *PLoS One* **3**, e1797 (2008).
- 600 39. Prinster, S. C., Hague, C. & Hall, R. A. Heterodimerization of G Protein-Coupled Receptors :
601 Specificity and Functional Significance. **57**, 289–298 (2005).
- 602 40. Wellman, M. & Abizaid, A. Growth Hormone Secretagogue Receptor Dimers: A New
603 Pharmacological Target. *eneuro* (2015).
- 604 41. Egecioglu, E. *et al.* Ghrelin increases intake of rewarding food in rodents. *Addict. Biol.* **15**,
605 304–311 (2010).
- 606

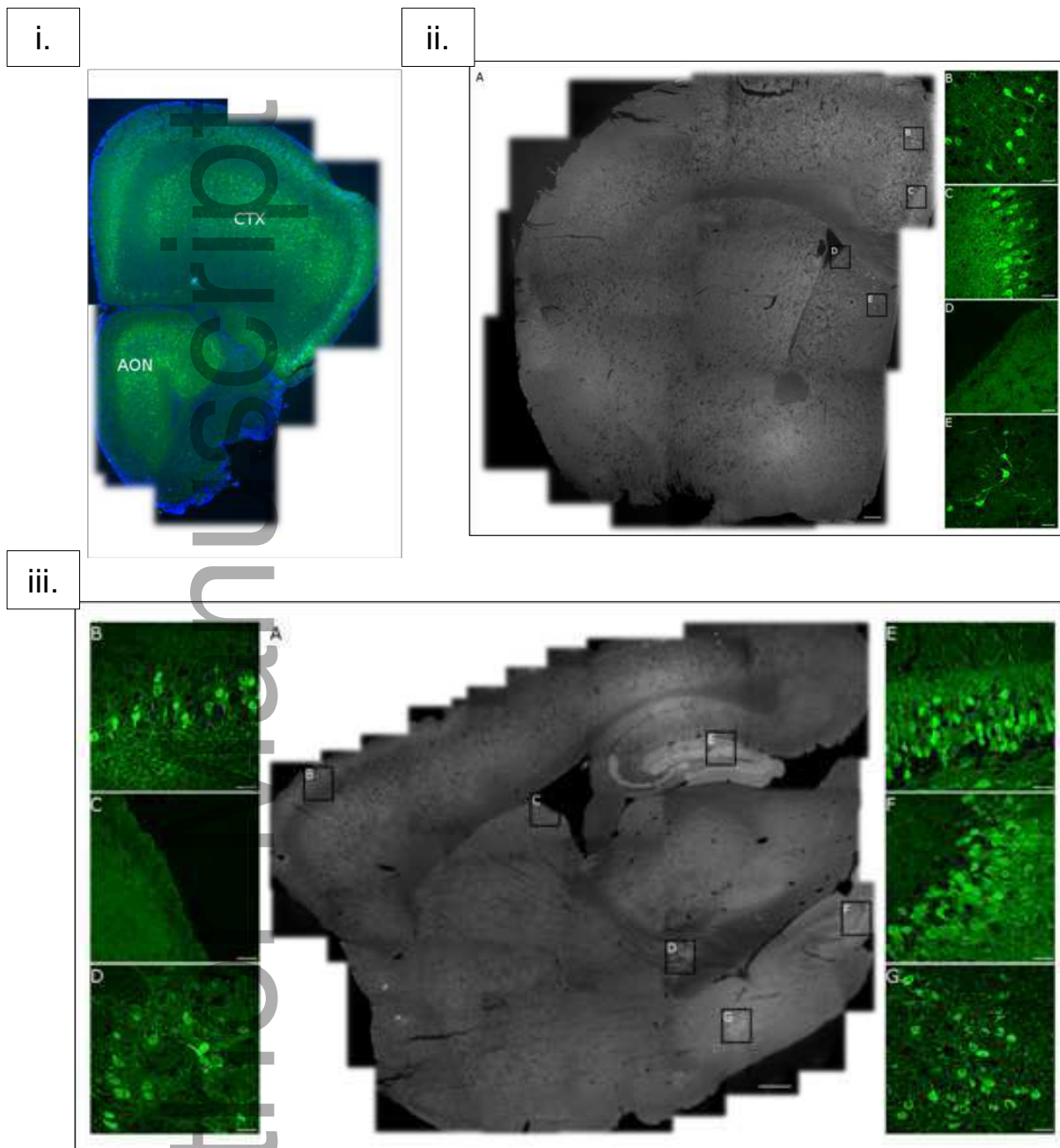
Figure 1. Ratcliff *et al.*

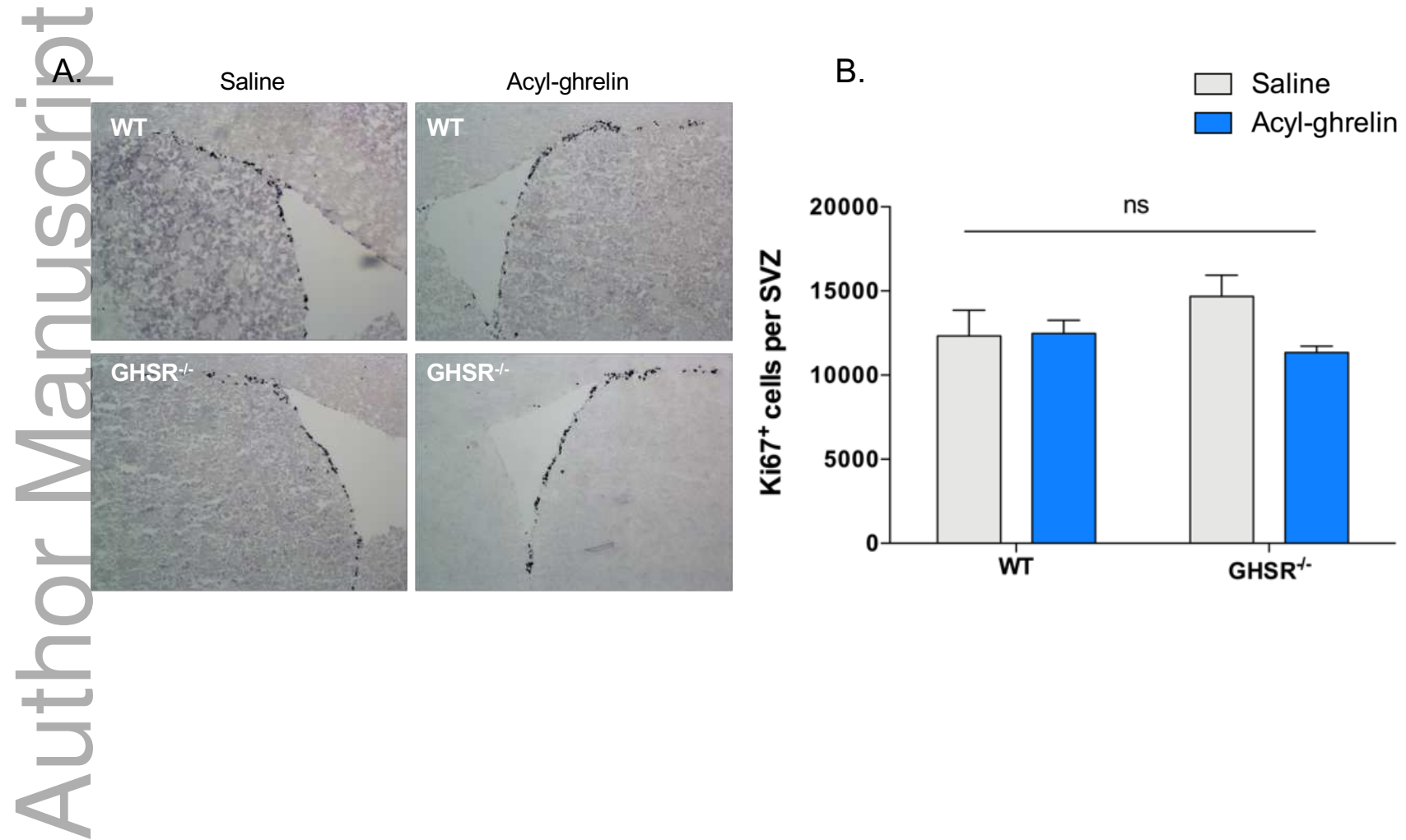
Figure 2. Ratcliff *et al.*

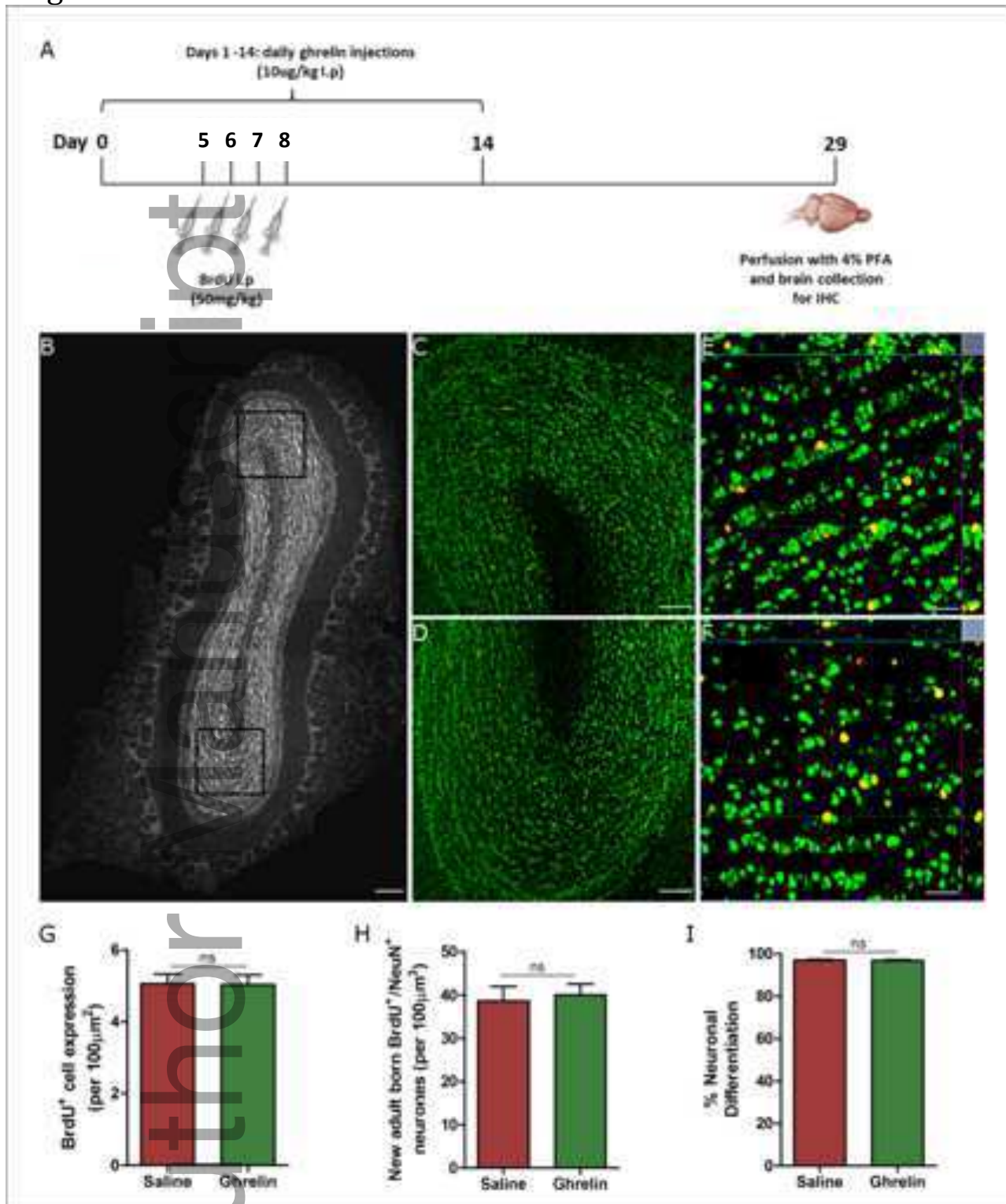
Figure 3. Ratcliff *et al.*

Figure 4. Ratcliff *et al.*